AIP | Conference Proceedings

Characterization of die drool sample produced by HDPE melt extrusion

Jan Musil and Martin Zatloukal

Additional information on AIP Conf. Proc.

Characterization of Die Drool Sample Produced by HDPE Melt Extrusion

Jan Musil[a] and Martin Zatloukal[a,b]

[a]Centre of Polymer Systems, University Institute, Tomas Bata University in Zlin,
Nad Ovcirnou 3685, 760 01 Zlin, Czech Republic
[b]Polymer Centre, Faculty of Technology, Tomas Bata University in Zlin,
nam. T. G. Masaryka 275, 762 72 Zlin, Czech Republic

Abstract. In this work, flow induced molecular weight fractionation experiment was performed for HDPE polymer on specially designed laboratory extrusion setup. Die drool sample, accumulated at the die exit face, together with virgin pellets were consequently characterized experimentally by gel permeable chromatography, differential scanning calorimetry and rheology as well as theoretically by recently proposed generalized Newtonian model.

INTRODUCTION

During flow of viscoelastic polymer melts, flow induced molecular weight fractionation (redistribution of macromolecules according to their molecular weights) inside a flow channel can occur due to presence of highly inhomogeneous stress field profile.

Historically, the first notice about polymer melt spontaneously fractionating during flow under inhomogeneous stresses in capillary was presented in 1964 by Busse [1]. On the theoretical level he claimed that "capillary viscometer should tend to fractionate polymer molecules with respect to molecular weight along the radius of the capillary." His original imagination assumed that "near the wall, molecules of high molecular weight acquire relatively large amounts of free energy of elastic deformation, while very small molecules do not. Hence, there is a thermodynamic force that tends to increase the concentration of very small molecules at the wall, and of the larger molecules nearer the axis."

One year later, Schreiber and Storey [2] experimentally tested this energy based theory on three different polyethylene samples. First was low density polyethylene, second and third were blends of linear polyethylenes with broad and narrow molecular weight distribution, respectively. Static light scattering showed significant reduction of molecular weight in a surface layer for the first sample and, more pronounced, for the second one. On the other hand, the third sample showed no marked fractionation. They also tested dies with different length/diameter (*L/D*) ratios and they found that

magnitude of the fractionation effect increases with increasing *L/D*. With these results, authors consequently developed a simple mathematical model for flow induced molecular weight fractionation [3].

With the assumption that molecular weight fractionation during shear flow is thermodynamical phenomenon, Schreiber [4] investigated extruded parts in different layers (from the centerline to the skin) by calorimetry as well as extrudate swelling method. Again, the conclusion was that "the molecular redistribution which we have observed is a feature of crystallizable polymers with very wide molecular weight distributions."

In 1972, Whitlock and Porter [5] performed similar tests with broad distribution polystyrene melt. However, even under widely varying conditions of shear rate, shear stress, and temperature, they observed no significant molecular weight fractionation. In order to explain this anomaly, Tirrel and Malone [6] developed stress-induced diffusion mathematical model. Based on their modelling results, they believed that the flow conditions were not optimal for appearance of a measurable fractionation degree, but that fractionation could be significant under proper flow conditions. Unfortunately, after this little failure, no more research papers focused on flow induced molecular weight fractionation in polymer melts in the next more than quarter-century have been published.

Nevertheless, idea of this type of molecular fractionation has been recently rediscovered [7]. Authors extruded polyethylene terephthalate (PET) as a thin film and then, the film milled down in small increments and collected the shavings at each single step for later GPC analysis. The results show a gradient in the concentration of molecular weight across the film thickness. Again, the trend is the same as in the former Schreiber's work. Thus, molecular weight decreases from centreline towards to the wall. Moreover, authors speculated that "if the hypothesis that shear fields can serve to fractionate polymer melts is true, it could help to explain a number of common polymer processing problems…as…plateout of low molecular weight oligomer on metal surfaces or drooling of low molecular weight material from die lips."

Finally, in our recently published papers [8-10] focused on flow induced molecular weight fractionation during extrusion of unfilled and well-stabilized HDPEs at very low processing temperature was found that molecular weight distribution curves for HDPE extrudate skin, extrudate core and for virgin pellets are practically identical and the die drool sample represents their low molecular weight fraction, which suggests that in this case the internal die drool phenomenon (spontaneous accumulation of extruded polymer melt on die exit faces) can be considered to be the result of the flow induced molecular weight fractionation taking place only in a very thin layer near the die wall (within less than 8% of the channel radius for the studied processing conditions) and the extrusion process itself has no effect on the polymer bulk. Further, it has been revealed that the low molecular weight polymer chains start to be fractionated from the main polymer melt stream under the slip-stick flow instability regime which consequently then accumulates at the die lips in the form of a low viscosity polymer melt. It has also been found that increase in HDPE melt elasticity by the controlled increase in a small amount of very long linear chains of HDPE polymer (i. e. while keeping the polydispersity index constant), leads to more effective flow

induced fractionation resulting in narrow molecular weight distribution of the die drool sample containing a small amount of long chains.

In this work, die drool sample carefully collected from die exit face during HDPE extrusion process together with virgin pellets were characterized experimentally as well as theoretically in order to explore available data needed for further fundamental understanding of die drool phenomenon.

EXPERIMENTAL

The experimental work is divided into two following parts. As the first, extrusion of chosen HDPE polymer melt on specially designed laboratory extrusion setup during which accumulated die drool material on the die exit face is carefully collected. Then, as the second, material characterization (gel permeable chromatography, differential scanning calorimetry and rheology) of virgin pellets as well as collected die drool is performed.

Samples Preparation

Unfilled, well-stabilized and virtually linear HDPE polymer melt (HDPE Liten FB 29 E2009 3220 4479, extrusion grade, Unipetrol RPA, Czech Republic) was extruded on specially designed laboratory extrusion line (in detail presented in [8,9]) at following processing conditions. Temperature profile along the screw was: $T_1 = 150°C$, $T_2 = 155°C$, $T_3 = 160°C$, $T_4 = 160°C$. Transition part and die were heated on $T_5 = 160°C$ and $T_6 = 160°C$. Extrudate mass flow rate was 731 g.hr^{-1} (corresponding apparent shear rate 652 s^{-1}) and die drool mass flow rate was 0.3462 g.hr^{-1} (corresponding dimensionless buildup ratio BR [11] defined as drool mass flow rate divided by extrudate mass flow rate was 0.0004733427). These conditions were set due to highly pronounced fractionation effect inside the die and high die drool mass accumulation on die exit face [9]. Die drool mass was collected after 10 minutes of extrusion and total weight was approximately 1.5 g. Then, samples for rotational and extensional rheology were prepared by compression moulding and special cutters.

Material Characterization

Molecular weight averages (M_n, M_w, M_z and M_{z+1}) as well as molecular weight distributions were determined by PL-GPC 220 model (Polymer Laboratories, United Kingdom) equipped with refractometric detector PL-220 DRI for all samples (virgin pellets, bulk extrudate and die drool). Mobile phase was 1,2,4-trichlorbenzene HPLC grade (Scharlau, Spain) stabilized by 0.025% Santonox R (flow rate: 1 ml.min^{-1}). Each polymer sample was prepared as 1 mg dissolved in 1 ml of mobile phase and it was measured two times. Testing temperature was 160°C.

Thermal properties (peak melting and glass transition temperatures, heat of fusion and crystallinity) were determined by differential scanning calorimetry (NETZSCH DSC 200 PC) in temperature range of -150°C up to 350°C (temperature step 10°C per minute) under inert N_2 atmosphere.

Linear viscoelastic properties (storage modulus, G', loss modulus, G'' and complex viscosity, η^*) were measured on Advanced Rheometric Expansion System (ARES 2000 model, Rheometrics Scientific, USA) in parallel plates mode (plates diameter of 25 mm) within 0.1 rad.s^{-1} up to 100 rad.s^{-1} frequency range at 1% shear strain to guarantee linear viscoelasticity regime only. In order to capture Newtonian plateau, linear viscoelastic properties were measured at temperature step of 20°C within 130-370°C (virgin pellets) and 130-310°C (die drool sample) temperature range, which represents 13 and 10 single measurements in total, respectively. It should be noted that all measurements over 190°C were done under inert N_2 gas atmosphere to prevent possible polymer sample thermo/oxidative degradation. Finally, temperature superposition principle was used to create master curve at one reference temperature 190°C.

Transient extensional viscosity, η_E, was determined at 190°C on Sentmanat Extensional Rheometer (SER-HV-A01 model, Xpansion Instruments, USA [12-15]) attached to ARES 2000 rotational rheometer. The samples width was fixed to be 12.7 mm (done by calibrated dual blade cutter) and thickness approximately 0.5 mm (measured before each single test by micrometer). It should be noted that 'steady state' extensional viscosity data were taken from the peaks appearing on the transient viscosity curves for corresponding extensional strain rates.

Constitutive Equation

In order to describe basic rheological data for both tested samples, recently proposed generalized Newtonian fluid model has been utilized [16,17]:

$$\tau = 2\eta\left(I_{|D|}, II_D, III_D\right)D \tag{1}$$

where τ means the extra stress tensor, D represents the deformation rate tensor and η stands for the viscosity, which is not constant (as in the case of standard Newtonian law), but it is allowed to vary with the first invariant of the absolute value of deformation rate tensor $I_{|D|} = tr(|D|)$, (where $|D|$ is defined as the square root of D^2) as well as on the second $II_D = 2tr(D^2)$, and third, $III_D = \det(D)$, invariants of D according to Eq. 2

$$\eta\left(I_{|D|}, II_D, III_D\right) = A^{1-f\left(I_{|D|}, II_D, III_D\right)} \eta\left(II_D\right)^{f\left(I_{|D|}, II_D, III_D\right)} \tag{2}$$

where $\eta(II_D)$ is given by the well-known Carreau-Yasuda model (Eq. 3) and $f\left(I_{|D|}, II_D, III_D\right)$ is given by Eq. 4.

$$\eta(II_D) = \frac{\eta_0 a_T}{\left[1 + \left(\lambda a_T \sqrt{II_D}\right)^a\right]^{\left(\frac{1-n}{a}\right)}} \tag{3}$$

50

$$f\left(I_{|D|}, II_D, III_D\right) = \left\{ \tanh\left[\alpha a_T \left(1 + \frac{1}{4\left(\sqrt{3}\right)^3}\right)^{-\psi} \left(\left|1 + \frac{III_D}{II_D^{3/2}}\right|\right)^{\psi} \frac{\sqrt[3]{4|III_D|} + I_{|D|}}{3} + \beta \frac{1}{\tanh(\beta)} \right] \right\}^{\zeta} \quad (4)$$

here A, η_0, λ, a, n, α, ψ, β, ζ are adjustable parameters and a_T is temperature shift factor defined by the Arrhenius equation:

$$a_T = \exp\left[\frac{E_a}{R}\left(\frac{1}{273.15 + T} - \frac{1}{273.15 + T_r} \right) \right] \quad (5)$$

where E_a is the activation energy, R is the universal gas constant, T_r is the reference temperature and T is local temperature.

Results and Discussion

As the first, basic material properties for virgin pellets and die drool sample are summarized in Table 1 (density and melt flow index for die drool sample were not measured).

TABLE 1. Basic material properties for virgin pellets and die drool sample.

		Virgin pellets	Die drool sample
Density	$(g.cm^{-3})$	0.95*	-
M_n	$(g.mol^{-1})$	17,045	14,585
M_w	$(g.mol^{-1})$	239,300	84,020
M_z	$(g.mol^{-1})$	1,613,000	340,450
M_{z+1}	$(g.mol^{-1})$	3,476,000	951,400
M_w/M_n	(-)	14.04	5.80
Melt flow index (190°C/2.16kg)	$(g.10min^{-1})$	0.15*	-
Zero-shear rate viscosity	(Pa.s)	985,825	4,132
Flow activation energy	$(kJ.mol^{-1})$	16.301	15.207
DSC peak melting point	(°C)	131.8	131.3
Glass transition temperature	(°C)	-130.9	-133.0
DSC heat of fusion	$(J.g^{-1})$	213.2	213.9
Crystallinity	(%)	72.76	73.00

* Taken from the original material data sheet for basic polymer HDPE Liten FB 29.

Then, molecular weight distribution curves for virgin pellets, bulk extrudate and die drool sample are shown in Figure 1. As can be seen, virgin pellets and bulk extrudate have virtually same molecular weight distributions. Due to this, following DSC and rheology measurements were done for virgin pellets and die drool sample only. Moreover, as can be clearly seen, die drool sample represents low molecular weight fraction of extruded polymer melt.
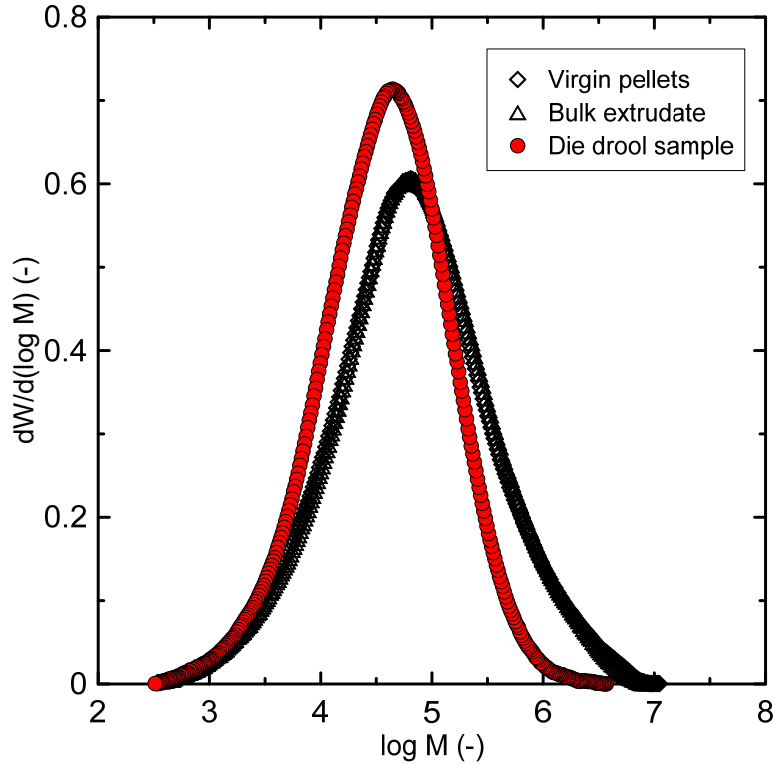
FIGURE 1. Molecular weight distribution curves for virgin pellets, bulk extrudate and die drool sample.
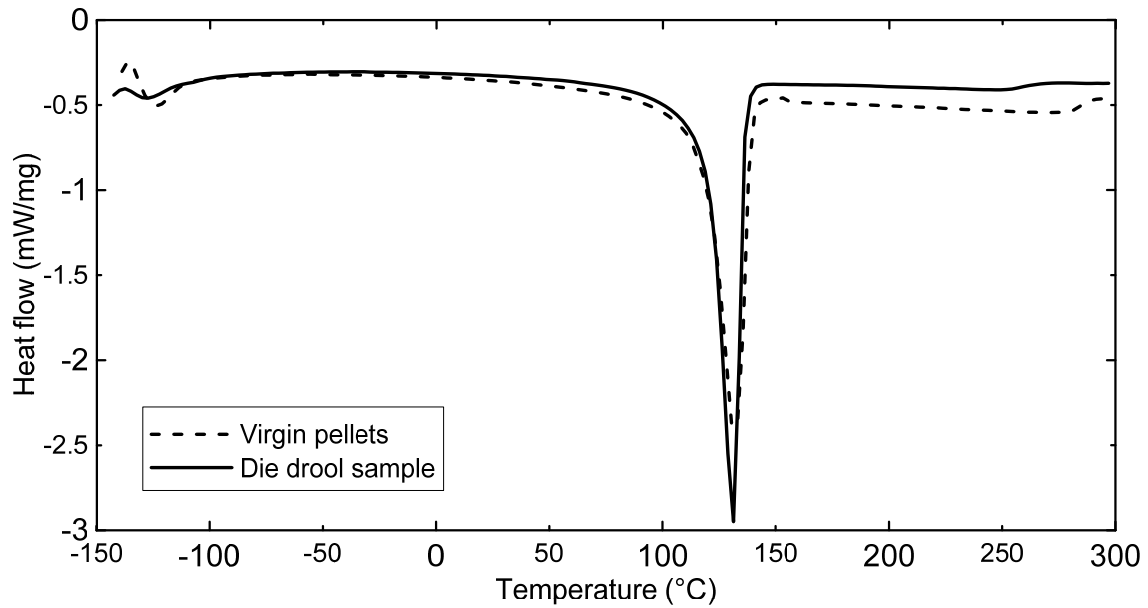

FIGURE 2. DSC curves for virgin pellets and die drool sample.

Thermal properties of virgin pellets and die drool sample are shown in Figure 2. Die drool as low molecular weight material has less pronounced glass transition region and narrower melting peak than virgin pellets. Peak melting temperatures, heats of fusion and crystallinities are virtually the same for both samples.

52

Rheological characterization of virgin pellets and die drool sample were determined at one reference temperature 190°C in order to emphasize their differences and the results are provided in Figures 3-7. It is clearly visible that zero-shear rate viscosity, uniaxial extensional viscosity and relaxation time for virgin pellets is much higher in comparison with die drool sample. Further, both samples can be considered as virtually linear materials because of no strain hardening peaks appear on their uniaxial extensional viscosity curves. Finally, the utilized generalized Newtonian model has very good capability to describe strain rate dependent steady-state shear and uniaxial extensional viscosities as shown in Figure 7 (model parameters are provided in Table 2).
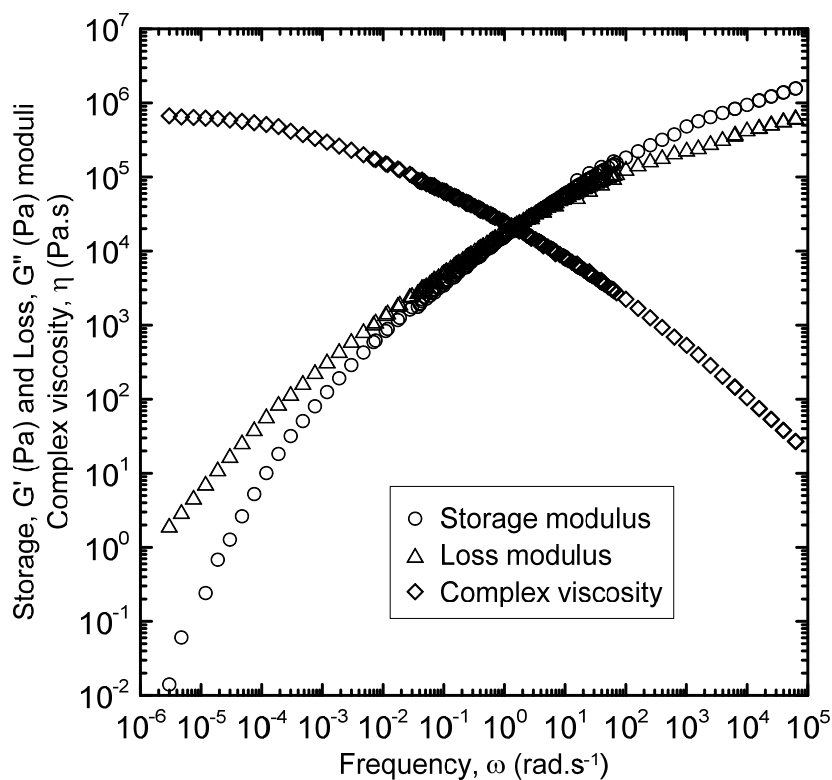

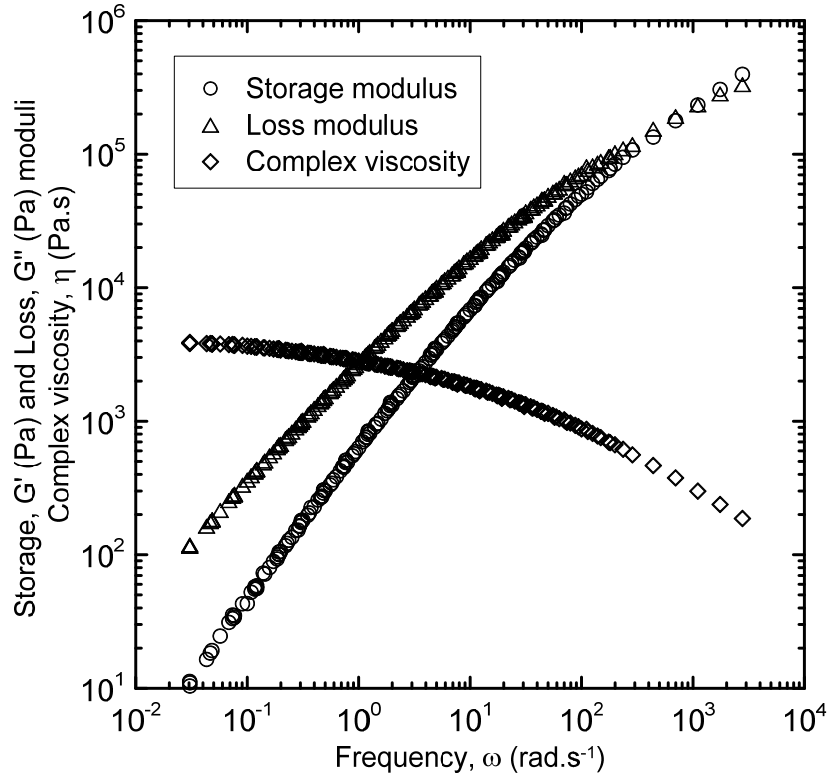**FIGURE 3.** Linear viscoelastic properties for virgin pellets at 190°C.

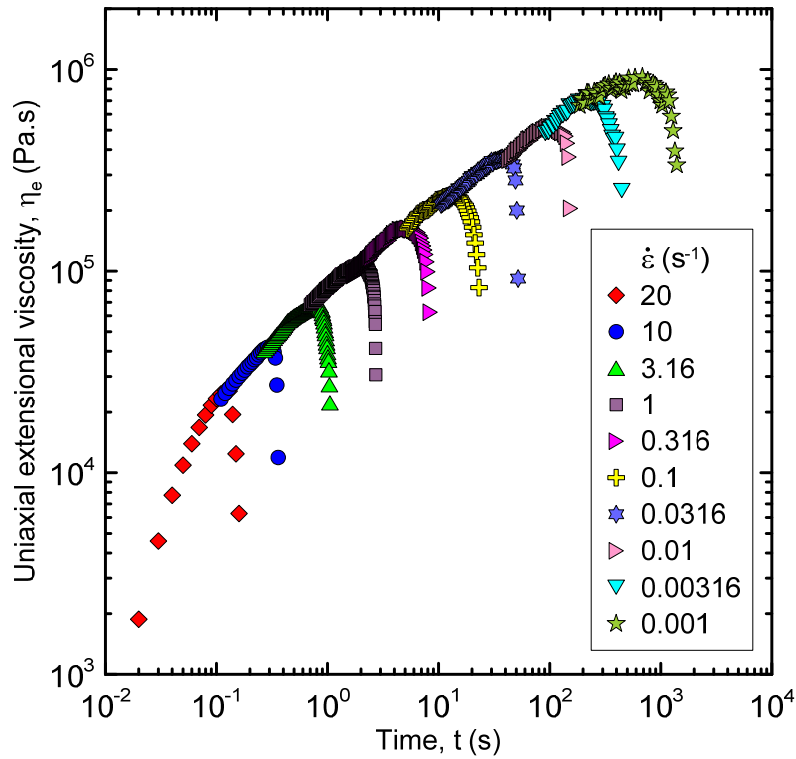**FIGURE 4.** Linear viscoelastic properties for die drool sample at 190°C.

FIGURE 5. Transient uniaxial extensional viscosity for virgin pellets at 190°C.
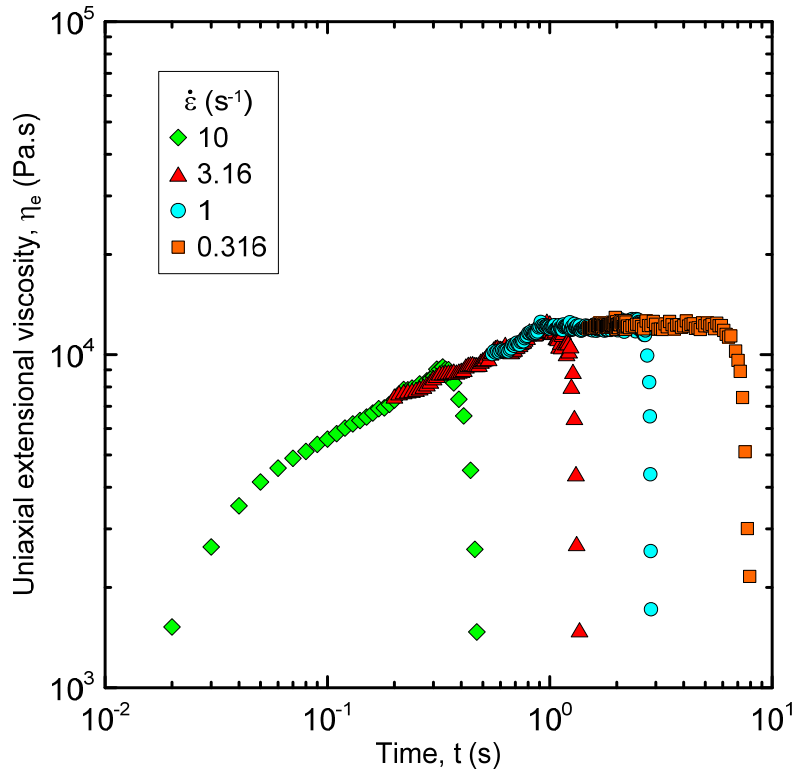
54

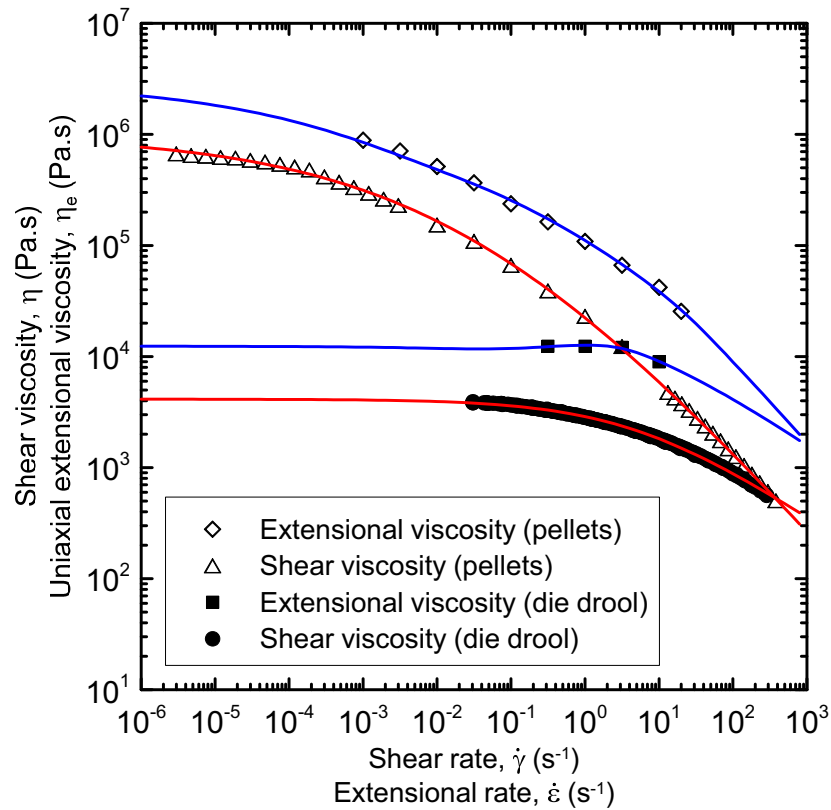**FIGURE 6.** Transient uniaxial extensional viscosity for die drool sample at 190°C.

FIGURE 7. Steady-state shear and uniaxial extensional viscosities for virgin pellets and die drool sample together with generalized Newtonian model fit (solid lines) at 190°C.

55

TABLE 2. Generalized Newtonian model parameters.

	Virgin pellets	Die drool sample
η_0 (Pa.s)	985,825	4,132
λ (s)	27.1500	0.1868
a (-)	0.2398	0.4707
n (-)	0.2204	0.5461
α (s)	0.05434	0.38717
β (-)	0.000336	0.049300
ζ (-)	0.003429	0.004968
ψ (-)	20	20
A (Pa.s)	$2\cdot10^{-16}$	$2\cdot10^{-16}$

Moreover, in order to evaluate wall slip for investigated HDPE material, slip velocity as function of shear stress was determined from the differences between complex modulus (G^*) calculated from storage (G') and loss (G'') moduli according to Eq. 6 from oscillatory measurements and corrected shear stress (τ_w) measured on capillary rheometer according to Eq. 7.

$$G^* = \sqrt{G'^2 + G''^2} \tag{6}$$

$$v_s(\tau_w) = \frac{D}{8}\left[\dot{\gamma}(\tau_w) - \omega\left(\left|G^*\right|\right)\right] \tag{7}$$

where D is capillary diameter, as suggested in [18,19]. Here, capillary with diameter 0.5 mm and $L/D = 16$ was used.
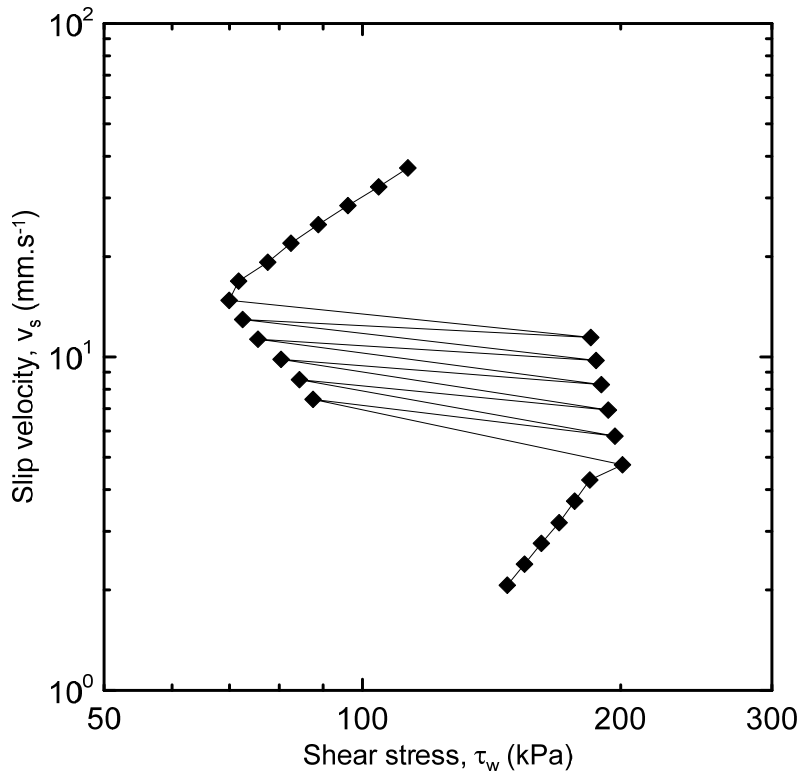

FIGURE 8. Slip velocity versus shear stress for investigated virgin pellets at 160°C.

56

The slip velocity versus shear stress dependence is depicted in Figure 8. Parameters in slip function (Eq. 8) were calculated from data points above slip-stick region, i.e. at the "superflow" regime where full slip takes place.

$$v_\text{s} = 30.1856\tau_\text{w}^{1.7261} \tag{8}$$

where units for slip velocity v_s and shear stress τ_w are (mm.s^{-1}) and (kPa/100), respectively.

CONCLUSION

In this work, flow induced molecular weight fractionation experiment was performed for HDPE polymer on specially designed laboratory extrusion setup and die drool sample together with virgin pellets were characterized by gel permeable chromatography, differential scanning calorimetry and rheology. It is believed that the obtained experimental data for HDPE can be used in the FEM flow modeling of die drool phenomenon at the die exit region in order to better understand the stabilizing/destabilizing role of the die exit region with respect to die drool phenomenon. For such purpose, the flow situation inside the extrusion die can be viewed as the special case of two-layer coextrusion at presence of significant slip where the low molecular weight species (formed due to flow induced fractionation) represents the low viscosity skin and the main polymer the high viscosity core.

ACKNOWLEDGMENTS

REFERENCES

1. W. F. Busse, *Phys. Today* **17**, 32-41 (1964).
2. H. P. Schreiber and S. H. Storey, *Polym. Letters* **3**, 723-727 (1965).
3. H. P. Schreiber, S. H. Storey and E. B. Bagley, *J. Rheol.* **10**, 275-297 (1966).
4. H. P. Schreiber, *J. App. Polym. Sci.* **18**, 501-508 (1974).
5. L. R. Whitlock and R. S. Porter, *J. Polym. Sci. Chem. Ed.* **10**, 877-886 (1972).
6. M. F. Tirrell and M. F. Malone, *J. Polym. Sci. Phys. Ed.* **15**, 1569-1583 (1977).
7. M. D. Shelby and G. B. Caflisch, *Polym. Eng. Sci.* **44**, 1283-1294 (2004).
8. J. Musil and M. Zatloukal, *Chem. Eng. Sci.* **66**, 4814-4823 (2011).
9. J. Musil and M. Zatloukal, *Chem. Eng. Sci.* **81**, 146-156 (2012).
10. J. Musil and M. Zatloukal, *Int. J. Heat Mass Tran.* **56**, 667-673 (2013).

11. J. D. Gander and A. J. Giacomin, *Polym. Eng. Sci.* **37**, 1113-1126 (1997).
12. M. L. Sentmanat, U.S. Patent No. 6,578,413 B2 (2003).
13. M. L. Sentmanat, U.S. Patent No. 6,691,569 B1 (2004).
14. M. L. Sentmanat, *Rheol. Acta.* **43**, 657-669 (2004).
15. M. L. Sentmanat, B. N. Wang and G. H. McKinley, *J. Rheol.* **49**, 585-606 (2005).
16. M. Zatloukal, *J. Non-Newtonian Fluid Mech.* **165**, 592-595 (2010).
17. M. Zatloukal, *Annual Technical Conference – ANTEC, Conference Proceedings* **1**, 92-96 (2011).
18. H. E. Park, S. T. Lim, F. Smillo and J. M. Dealy *J. Rheol.* **52**, 1201-1239 (2008).
19. Y. W. Inn, *J. Rheol.* **57**, 393-406 (2013).